Available online at www.sciencedirect.com
ScienceDirect
Catalysis Today 131 (2008) 559–565
CATALYSIS TODAY
www.elsevier.com/locate/cattod

Reaction kinetic for poly(styrene-*co*-vinylbenzyl chloride)-supported catalyst containing pendant tetraethylammonium chloride in the reaction of glycidyl methacrylate with carbon dioxide

S.W. Park [a,*], B.S. Choi [a], D.W. Park [a], S. Udayakumar [a], J.W. Lee [b]

[a] *Division of Chemical Engineering, Pusan National University, Busan 609-735, Republic of Korea*
[b] *Division of Chemical Engineering, Sogang University, Seoul 121-742, Republic of Korea*

Available online 26 November 2007

Abstract

A soluble copolymer-supported catalyst containing pendant triethylammonium chloride was synthesized by the radical copolymerization of *p*-chloromethylated styrene with styrene followed by the addition reaction of the resulting copolymer with triethylamine. Initial absorption rate of carbon dioxide into glycidyl methacrylate (GMA) solutions containing the catalyst was measured in a semi-batch stirred tank with a plane gas–liquid interface at 101.3 kPa. The reaction rate constants of the reaction between carbon dioxide and GMA were evaluated from analysis of the mass transfer mechanism accompanied by the elementary reactions based on the film theory. Solvents such as toluene, *N*-methyl-2-pirrolidinone, and dimethyl sulfoxide influenced on the reaction rate constants. Furthermore, this catalyst was compared to the monomeric tetraethylammonium chloride under the same reaction conditions.

Keywords: Glycidyl methacrylate; Immobilized tetraethylammonium chloride; Absorption; Carbon dioxide

1. Introduction

The chemical fixation of carbon dioxide has received much attention in view of environmental problems. An attractive strategy to deal with this situation is converting CO_2 into valuable substances [1]. The reaction of carbon dioxide with oxiranes leading to five-membered cyclic carbonates is well known [1]. These cyclic carbonates can be used as polar aprotic solvents, electrolytes for batteries and sources for reactive polymers [2].

The synthesis of cyclic carbonates by the reaction of CO_2 with oxirane has been performed using Lewis acids, transition metal complexes, and organometallic compounds as catalysts at high pressure such as 10–50 atm [3,4]. Some articles reported the synthesis of five-membered cyclic carbonates under mild conditions at atmospheric pressure in the presence of metal halides or quaternary onium salts [5–9].

Quaternary onium salts bound to polymer resins have been reported by several authors [6,8,9]. Most published works on resin-bound quaternary onium salts use styrene–divynyl benzene-related resins because many amount of technologies are available on these resins due to their use as an ion-exchange resin support [10]. The polymer-supported catalysts can be easily separated from reaction mixtures and can be reused.

The papers [3–9] about oxirane–CO_2 reactions have focused on the reaction mechanism, the overall reaction kinetics, and the effect of the catalyst on the conversion. But, because the diffusion may have an effect on the reaction kinetics [11] in the mass transfer accompanied by chemical reactions, we believe that it is worthwhile to investigate the effect that diffusion has on the reaction kinetics of the gas–liquid heterogeneous reaction such as the oxirane–CO_2 reaction.

In our previous works, we studied the kinetics in the reaction between CO_2 and phenyl glycidyl ether using Aliquat 336 [12], glycidyl methacrylate (GMA) using 18-crown-6 [13], Aliquat 336 [14], and tetrabutylammonium bromide [15] as a catalyst in series. They presented the reaction rate constants as a combined form using the pseudo-first-order reaction method based on the reaction mechanism [4] with two steps. The reaction rate

* Corresponding author. Tel.: +82 51 510 2393; fax: +82 51 512 8563.
E-mail address: swpark@pusan.ac.kr (S.W. Park).

0920-5861/$ – see front matter
doi:10.1016/j.cattod.2007.10.037

constants of the elemental reactions could not be obtained by the pseudo-first-order reaction method. In this study, the same reaction was performed using catalysts such as monomeric tetraethylammonium chloride (TEAC) and immobilized TEAC. We prepared the immobilized tetraethylammonium chloride catalyst (we call it as poly-cat) using a copolymer of styrene and vinylbenzyl chloride, and determined the reaction rate constants using the measured initial absorption rate of CO_2 and the mass transfer mechanism of CO_2 accompanied by chemical reactions. Effect of solvents such as toluene, *N*-methyl-2-pirrolidinone (NMP), and dimethyl sulfoxide (DMSO) on the catalytic activities was observed.

2. Theory

The overall reaction [7] between CO_2 (A) and GMA (B) using a catalyst (QX) at atmospheric pressure to form (2-oxo-1,3-dioxolan-4-yl)methacrylate (DOMA) is proposed as follows

$$CO_2 + GMA \rightarrow DOMA \tag{1}$$

The overall reaction in Eq. (1) with the rate-determining step of the attack of the anion part of the catalyst to GMA [7] is assumed to consist of two steps [4] as follows:

(i) A reversible reaction between B and QX to form an intermediate complex (C_1) and (ii) an irreversible reaction between A and C_1 to form QX and DOMA (C):

$$B + QX \underset{k_2}{\overset{k_1}{\leftrightarrow}} C_1 \tag{2}$$

$$A + C_1 \xrightarrow{k_3} C + QX \tag{3}$$

where k_1, k_2, and k_3 are the forward and backward reaction rate constant in reaction (2), and the reaction rate constant in reaction (3), respectively.

The reaction equilibrium constant (K_1) in the reversible reaction of Eq. (2) is defined as follows

$$K_1 = \frac{k_1}{k_2} = \frac{C_{C_1 eq}}{C_{Beq} C_{QXeq}} \tag{4}$$

It is assumed that species B and QX are nonvolatile and gas phase resistance to absorption is negligible by using pure species A, and thus, the concentration of species A at the gas–liquid interface corresponds to equilibrium with the partial pressure of species A in the bulk gas phase.

Under the assumptions mentioned above, the mass balances of species A, B, C_1, and QX using the film theory accompanied by chemical reactions and the boundary conditions are given as follows

$$D_A \frac{d^2 C_A}{dz^2} = k_3 C_{C1} C_A \tag{5}$$

$$D_B \frac{d^2 C_B}{dz^2} = k_1 C_B C_{QX} - k_2 C_{C1} \tag{6}$$

$$D_{C1} \frac{d^2 C_{C1}}{dz^2} = -k_1 C_B C_{QX} + k_2 C_{C1} + k_3 C_{C1} C_A \tag{7}$$

$$D_{QX} \frac{d^2 C_{QX}}{dz^2} = k_1 C_B C_{QX} - k_2 C_{C1} - k_3 C_{C1} C_A \tag{8}$$

$$z = 0; \quad C_A = C_{Ai}; \qquad \frac{dC_B}{dz} = 0, \quad \frac{dC_{C1}}{dz} = 0, \quad \frac{dC_{QX}}{dz} = 0 \tag{9}$$

$$z = z_L; \quad C_A = C_{AL}, \quad C_B = C_{BL}, \quad C_{C1} = C_{C_1 L}, \quad C_{QX} = C_{QXL} \tag{10}$$

The mass balance of QX is

$$Q_o = C_{QX} + C_{C1} \tag{11}$$

The enhancement factor (F) of A by chemical reaction is defined as ratio of the flux of A with reaction and that without reaction based on the film theory as follows

$$F = \frac{N_A}{N_{Ao}} = \left. \frac{-D_A (dC_A/dz)}{k_L (C_{Ai} - C_{AL})} \right|_{z=0} \tag{12}$$

If it is assumed that at the initial absorption rate of CO_2, C_B and C_{C_1} in the liquid film are constant as equilibrium concentrations (C_{Beq} and $C_{C_1 eq}$), which will be obtained in Section 4, and C_{Beq} is C_{Bo}, and then, Eqs. (5)–(8) become to be one differential equation as follows

$$D_A \frac{d^2 C_A}{dz^2} = k C_A \tag{13}$$

where

$$k = \frac{k_3 K_1 C_{Bo} Q_o}{1 + K_1 C_{Bo}} \tag{14}$$

F is derived from the exact solution of Eq. (13) and the definition of F in Eq. (12) as follows

$$F = \frac{\eta}{\tan h \eta} \tag{15}$$

where

$$\eta = \frac{\sqrt{k_3 K_1 D_A C_{Bo} Q_o / (1 + K_1 C_{Bo})}}{k_{Lo}} \tag{16}$$

Eq. (16) is rearranged as follows

$$\frac{Q_o}{(\eta k_{Lo})^2} = \frac{1}{k_3 D_A} + \frac{1}{k_3 D_A K_1 C_{Bo}} \tag{17}$$

The values of k_3 and K_1 are obtained from the plots of left side of Eq. (17) vs. $1/C_{Bo}$, where η comes from Eq. (15) using the measured F.

3. Experimental

3.1. Chemicals

All chemicals were of reagent grade and were used without further purification. Purity of both CO_2 and N_2 was more than

Table 1
Physical properties of CO_2/GMA/poly-cat and TEAC system

Temperature (°C)	Solvent	μ (cp)	C_{Ai} (kmol/m^3)	$D_A \times 10^9$ (m^2/s)	$D_B \times 10^9$ (m^2/s)	$D_{C_1} \times 10^9$ (m^2/s)	$k_{Lo} \times 10^5$ (m/s)
80	Toluene	0.362(0.322)	0.0783	8.683(9.379)	3.393(3.665)	1.977(2.136)	2.893(3.125)
	NMP	0.875(0.848)	0.0711	3.618(3.694)	1.414(1.444)	0.892(0.890)	1.798(1.836)
	DMSO	0.986(0.857)	0.0612	2.955(3.245)	1.155(1.268)	0.662(0.727)	1.340(1.472)
85	Toluene	0.351(0.307)	0.0727	9.133(9.977)	3.568(3.898)	2.054(2.246)	3.310(3.616)
	NMP	0.831(0.797)	0.0679	3.877(3.986)	1.515(1.558)	0.928(0.954)	1.861(1.914)
	DMSO	0.950(0.808)	0.0576	3.132(3.490)	1.224(1.364)	0.692(0.771)	1.702(1.897)
90	Toluene	0.334(0.294)	0.0698	9.704(10.56)	3.792(4.128)	2.192(2.387)	3.692(4.019)
	NMP	0.772(0.750)	0.0629	4.2134.295)	1.646(1.678)	1.016(1.036)	2.307(2.352)
	DMSO	0.863(0.764)	0.0544	3.452(3.743)	1.349(1.463)	0.783(0.849)	2.025(2.196)

Numbers in parentheses are the physical properties for TEAC.

99.9%. GMA, styrene (ST), vinylbenzyl chloride (VBC), and 2,2′-azobisisobutylonitrile (AIBN) were supplied by Aldrich Chemical Company, USA.

3.2. Absorption procedure

A semi-batch stirred tank (0.075 m inside diameter, 0.13 m height, agitation speed of 50 rpm) with a plane gas–liquid interface was used to measure the outlet flow rate of CO_2 using a mass flow meter (Brook Instrument, USA) in GMA solutions in range of 0.5–3 kmol/m^3 with catalyst at temperature in the range of 80–90 °C. A condenser was attached to the absorber to prevent the effluent vapors of GMA and solvents. The concentration of CO_2 in the bulk body of the liquid (C_{AL}) at a given absorption time was obtained from the difference of the inlet and outlet flow rate of gas of the absorber [16]. The flow rate of CO_2 at the inlet was maintained at 50 cm^3/min. The experimental procedure used to obtain the absorption rate of CO_2 was identical to that described earlier [15].

3.3. Preparation of catalyst

Copolymer of ST and VBC was synthesized by the radical copolymerization of VBC (31.3 mol%) with ST (68.7 mol%) using AIBN as an initiator in toluene at 60 °C for 5 h, and then at 80 °C for 2 h under nitrogen gas, followed by precipitation into methanol and two reprecipitations from tetrahydrofuran (THF) solution into methanol. The VBC unit in the synthesized copolymer was measured by ^{1}H NMR and its value was 41 mol%. The copolymer was reacted with triethylamine in dimethylformamide (DMF) at 80 °C for 48 h.

The resulting polymer was purified by reprecipitating twice from methanol solution into diethyl ether, and dried at 50 °C under vacuum to obtain the catalyst. The attached amount of N^+ in the catalyst was measured by the elemental analysis and its value was 1.46 mmol/g catalyst and the VBC unit with N^+ in the catalyst was calculated and its value was 26 mol%. The preparation procedure to obtain the soluble polymer-supported catalyst containing pendant tetraethylammonium chloride residue was reported elsewhere [17].

3.4. Physical properties of CO_2 and GMA

Solubility (C_{Ai}) of CO_2 in organic solvents such as toluene, NMP, and DMSO at 101.3 kPa was obtained by measuring the pressure difference of CO_2 before and after equilibrium between gas and liquid phase, similar to the procedure reported elsewhere [18]. Diffusivity (D_A, D_B, D_{C_1}) of CO_2, GMA, and C_1 in solvent was estimated from Wilke–Chang equation [19]. Viscosity (μ) of solvent was measured with Cannon–Fenske viscometer. The viscosity of solvent, solubility, mass transfer coefficient of CO_2, diffusivities of CO_2, GMA, and C_1 are listed in Table 1. Numbers in parenthesis are those for TEAC.

3.5. Analysis of DOMA

The presence of DOMA, which was produced from the reaction between CO_2 and GMA using poly-cat and TEAC, respectively, was confirmed to be the same by instrumental analysis, such as FT-IR (cyclic carbonate C=O peak at 1800 cm^{-1}) and ^{13}C NMR (cyclic carbonate C=O at 160 ppm) spectra, which were as same as those measured in previous studies [15].

4. Results and discussion

The procedure employed to determine k_L is based on measuring the amount of gas absorbed, according to the following equation:

$$\frac{dC_{AL}}{dt} = k_L a_V (C_{Ai} - C_{AL}) \quad (18)$$

where a_v is the specific contact area at the gas–liquid interface, and its value was 14.287 m^2/m^3.Integrating Eq. (18), the graphical representation of ln $[C_{Ai}/(C_{Ai} - C_{AL})]$ vs. time is obtained from the following equation.

$$\ln \frac{C_{Ai}}{(C_{Ai} - C_{AL})} = k_L a_V t \quad (19)$$

Fig. 1 shows typical plots of measured flow rate of gas at outlet against the absorption time in DMSO solution of GMA containing poly-cat and TEAC of 0.01 kmol/m^3, respectively, at 85 °C. As shown in Fig. 1, the measured flow rate increases

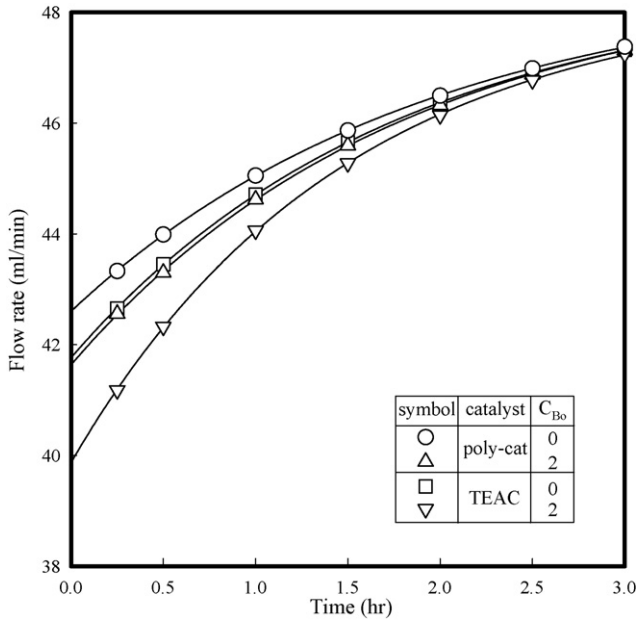

Fig. 1. Flow rate of gas at outlet vs. time in DMSO solution of GMA at $Q_o = 0.01$ kmol/m^3 and 85 °C.

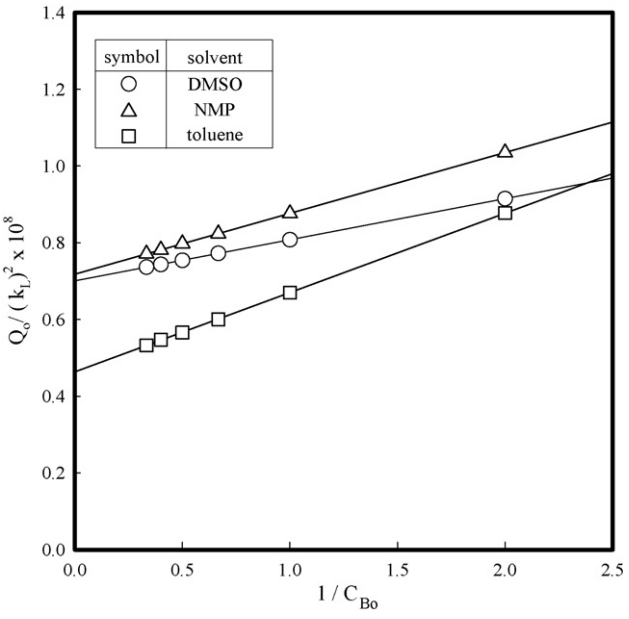

Fig. 3. $Q_o/(\eta k_L)^2$ vs. $1/C_{Bo}$ for various solvents.

with increasing the absorption time, and decreases with increasing the GMA concentration. Also, the flow rate using poly-cat is larger that that using TEAC.

Fig. 2 is a typical plot of ln $[C_{Ai}/(C_{Ai} - C_{AL})]$ vs. time under the same experimental conditions as those listed in Fig. 1. The plots in Fig. 2 shows straight lines through the origin, from the slope of which k_L were obtained. The mass transfer coefficients without a chemical reaction (k_{Lo}) are listed in Table 1.

Generally, the experimental F due to the chemical reaction in gas absorption is obtained as the ratio of the absorption rate with reaction to that without reaction in a continuous absorber,

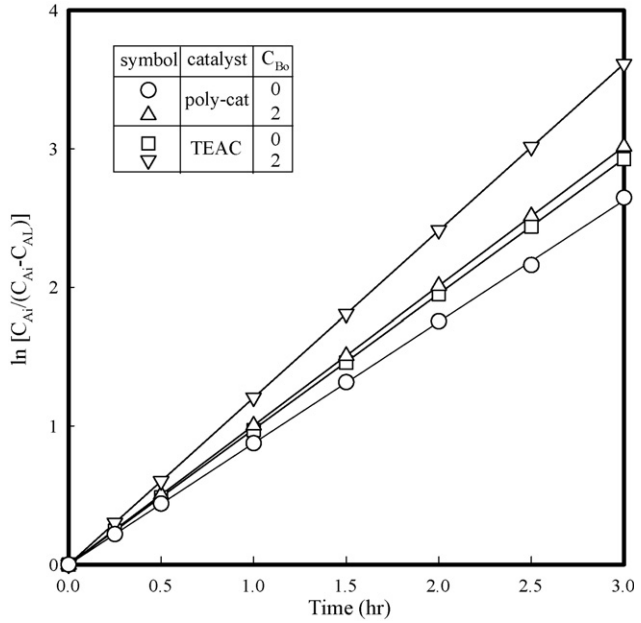

Fig. 2. ln $[C_{Ai}/(C_{Ai} - C_{AL})]$ vs. time under the same condition listed in Fig. 1.

or the ratio of the liquid-side mass transfer coefficient (k_L) of gas with reaction to that (k_{Lo}) without reaction [20] in a semi-batch absorber. F in this study was obtained from the ratio of k_L to k_{Lo}. And then, the value of η was obtained from Eq. (15) using the experimental F.

Fig. 3 shows plots of $Q_o/(\eta k_L)^2$ against $1/C_{Bo}$ for various solvents with poly-cat of 0.01 kmol/m^3 at 85 °C; these plots satisfy straight lines. The values of k_3 and K_1 were obtained from the intercept and slope of these straight lines. The values of k_3 and K_1 in toluene, NMP and DMSO at 85 °C were 2.363 m^3/(kmol s), 2.24 m^3/kmol, 3.59 m^3/(kmol s), 4.547 m^3/kmol, 4.557 m^3/(kmol s) and 6.546 m^3/kmol, respectively, which are listed in Table 2. The conversions (x) of GMA are obtained from Eq. (23) using the values of K_1 for the above conditions, and their values are 3.2%, 3.1% and 2.9%, respectively. This means that C_{Beq} can be used as C_{Bo}.

As shown in the differential equations of Eqs. (5)–(8) and the boundary conditions of Eqs. (9)–(11), the physico-chemical properties and the values of C_{AL}, C_{BL}, and C_{C_1L} are required to solve the differential equations and to obtain the theoretical F at the given C_{Bo} and Q_o. The every value of the physico-chemical properties except k_1 is given in Tables 1 and 2. And the values of C_{AL}, C_{BL}, and C_{C_1L} in the boundary condition of Eq. (10) are obtained as follows.

If the diffusion rate of A is not smaller than the reaction rate and the amount of the dissolved A that reacts in the diffusion film adjacent to the phase boundary compared to that which reaches the bulk liquid phase in the unreacted state is negligible, the concentration of A in the bulk phase (C_{AL}) is a finite quantity [11]. C_{AL} can be obtained from the following equation:

$$k_L a(C_{Ai} - C_{AL}) = k_3 C_{C_1 eq} C_{AL} \quad (20)$$

Table 2
Rate constants, K_1 (m^3/kmol) and k_3 (m^3/kmol s) of CO_2/GMA/poly-cat and TEAC system

	Temperature (°C)					
	80		85		90	
	K_1 (m^3/kmol)	k_3 (m^3/(kmol s))	K_1 (m^3/kmol)	k_3 (m^3/(kmol s))	K_1 (m^3/kmol)	k_3 (m^3/(kmol s))
Toluene	1.055(2.159)	1.096(3.275)	2.224(3.557)	2.363(4.813)	4.708(6.013)	4.968(7.744)
NMP	2.934(3.246)	2.031(4.952)	4.547(6.117)	3.590(7.130)	8.896(9.581)	6.247(9.892)
DMSO	4.042(5.520)	3.050(6.490)	6.546(7.906)	4.557(8.152)	10.737(11.483)	6.938(10.923)

Numbers in parentheses are the reaction rate constants for TEAC.

At the initial time, C_{BL} and C_{C_1L} become to be C_{Beq} and C_{C_1eq}, which are shown as follows.

The equilibrium concentration of B (C_{Beq}) and C_1(C_{C_1eq}) in the reversible reaction of Eq. (2) are expressed as follows

$$C_{Beq} = C_{Bo}(1-x) \tag{21}$$

$$C_{C_1eq} = \frac{K_1 C_{Bo}(1-x)Q_o}{1+K_1 C_{Bo}(1-x)} \tag{22}$$

The conversion of $B(x)$ is obtained with the known value of K_1 as follows

$$K_1 = \frac{C_{Bo}x}{C_{Bo}(1-x)(Q_o - C_{Bo}x)} \tag{23}$$

The value of k_1 is adjusted by the trial and error method to obtain the minimum deviation between F calculated from Eq. (15) and the experimental F. The values of F are calculated according to the change of k_1 from the solution of Eqs. (5)–(8) and (15). The plots of calculated F vs. k_1 are shown in Fig. 4 under the typical condition of C_{Bo} = 3 kmol/m^3, Q_o = 0.01 kmol/m^3 in DMSO at 85 °C. Because F is very insensitive to k_1 when k_1 is bigger than five from Fig. 4 and the bigger value of k_1 than 80 m^3/(kmol s) with F of 1.1514 was required for F approaching to the experimental F of 1.1516, k_1 was chosen as 80 m^3/(kmol s) in this typical condition approximately.

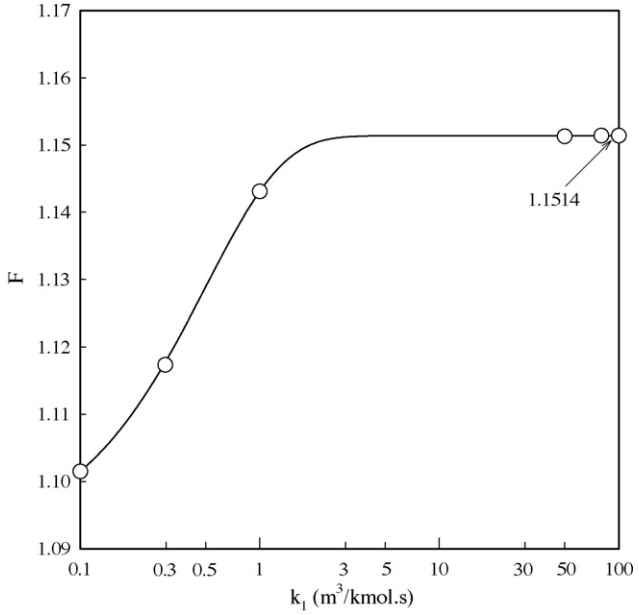

Fig. 4. F vs. k_1 at C_{Bo} = 3 kmol/m^3 in DMSO solution at 85 °C.

The concentrations of CO_2, GMA, C_1, and QX in the liquid film are obtained from the numerical solution of Eqs. (5)–(8) using the finite element method with the dimensionless parameters containing the adjusted k_1. At the typical condition of C_{Bo} = 0.5 kmol/m^3, Q_o = 0.01 kmol/m^3 in DMSO at 85 °C, the dimensionless concentration profiles of CO_2, GMA, C_1, and QX in the liquid film are illustrated in Fig. 5. The dimensionless parameters at the typical condition are listed in Fig. 5. As shown in Fig. 5, C_A and C_{QX} decrease, and C_B and C_{C_1} increase with increasing the depth of the liquid film (x).

To observe the effect of F on the concentration of GMA, absorption rates of CO_2 were measured according to changes of the GMA concentration over the range of 0.5–3 kmol/m^3 in each solvent. The plots of the experimental values of F against C_{Bo} are typically shown as open mark in Fig. 6. The solid line in Fig. 6 presents the calculated F, which is obtained using the

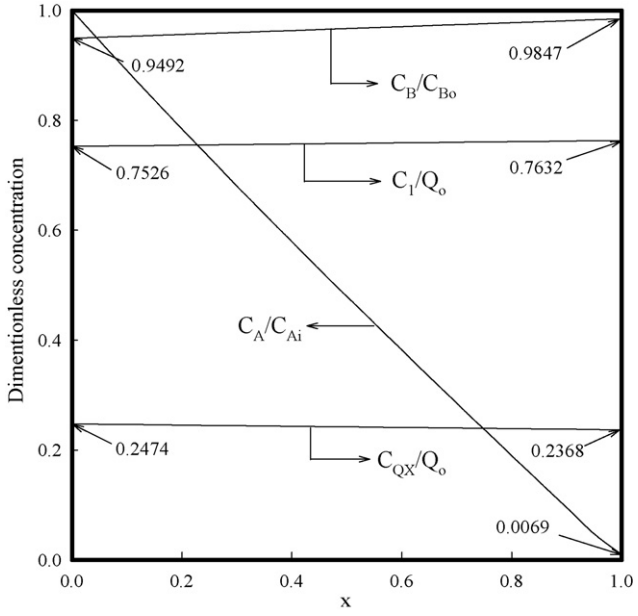

Fig. 5. Dimensionless concentration profile of CO_2, GMA, C_1 and QX in the liquid film under the condition such as C_{Bo} = 0.5 kmol/m^3, Q_o = 0.01 kmol/m^3 in DMSO at 85 °C. Dimensionless parameters: M = 0.4927, α = 17.557, β = 5.364, γ = 268.193, r_B = 2.5588, r_{C_1} = 4.5284, c_{AQ} = 5.76, c_{BQ} = 50, a_L = 0.0069, b_L = 0.9847 and c_{1L} = 0.7632.

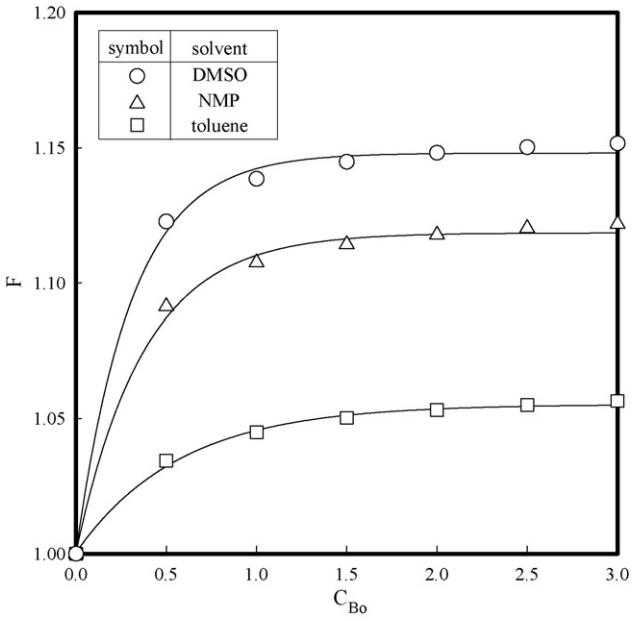

Fig. 6. F vs. C_{Bo} for various solvents with poly-cat of 0.01 kmol/m^3 at 85 °C.

procedure mentioned above. As shown in Fig. 6, F increases with increasing GMA concentration and increased in the order toluene, NMP, DMSO.

The rate reaction constants in organic reaction in a solvent generally reflect the solvent effect. Various empirical measurements about the solvent effect have been proposed to correlate with the reaction rate constant [21]. Some of them have a linear relationship to solubility parameter (δ) of solvent. Then, to observe δ on the reaction rate constant, the initial absorption rates of CO_2 were measured in solution of toluene, NMP and DMSO, respectively. Table 2 presents the values of k_3 and K_1 for various solvents and those for TEAC as numbers in parenthesis. Fig. 7 shows typically plots of logarithms of k_3 and K_1 vs. δ with poly-cat and TEAC using δ [22] of toluene, NMP and DMSO of 18.2, 23.1, and 24.6 (J/m^3)$^{0.5}$, respectively; the plots satisfy the linear relationship between the reaction rate constant and δ. The solvent polarity increases with increasing δ. It may be assumed that increased unstability and solvation of C_1 arising from the increased solvent polarity enhance the dissociation reaction of C_1 and the reaction between C_1 and CO_2, such as SN_1 (nucleophilic substitution) by solvation [23], respectively; thus, the values of K_1 and k_3 increase upon increasing δ, as shown in Fig. 7. This result coincides with that of Nishikubo et al. [9]. They presented that the yield of cyclic carbonate increased in the order toluene, NMP, DMSO in the addition reaction of 2-phenoxymethyloxirane with CO_2 using soluble polymer-supported catalyst with quaternary onium salt and explained the increase of the product with aprotic polarity.

To observe the effect of reaction temperature on the reaction rate constants, absorption rates of CO_2 were measured according to changes of the reaction temperature over the range of 80–90 °C. Table 2 presents the values of k_3 and K_1 for various temperatures. Fig. 8 shows typically plots of k_3 and K_1 against $1/T$ in a semi-logarithm scale in DMSO solution; the plots satisfy straight lines. The activation energy of reaction (3) was obtained from the slope of the plots for k_3; its value is 20.9 kcal/mol, and the heat of reaction (2), which was obtained from the slope of the plots for K_1; its value is 24.84 kcal/mol.

To compare the catalytic activity of poly-cat with that of the corresponding monomeric quaternary onium salt, k_3 and K_1 for TEAC of 0.01 kmol/m^3 were obtained using the same procedure as that for poly-cat and shown as numbers in parenthesis, and they are plotted vs. δ and $1/T$ in Figs. 7 and 8, respectively. As shown in Figs. 7 and 8, K_1 and k_3 for poly-cat

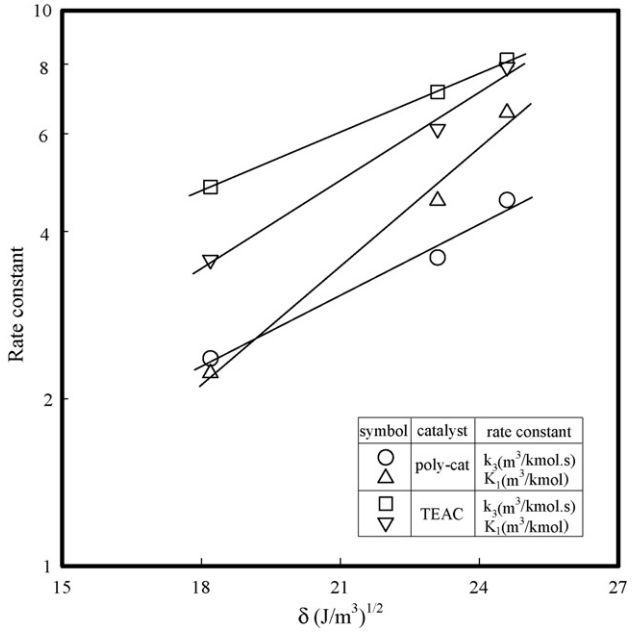

Fig. 7. Relationship between reaction rate constant and solubility parameter of solvent.

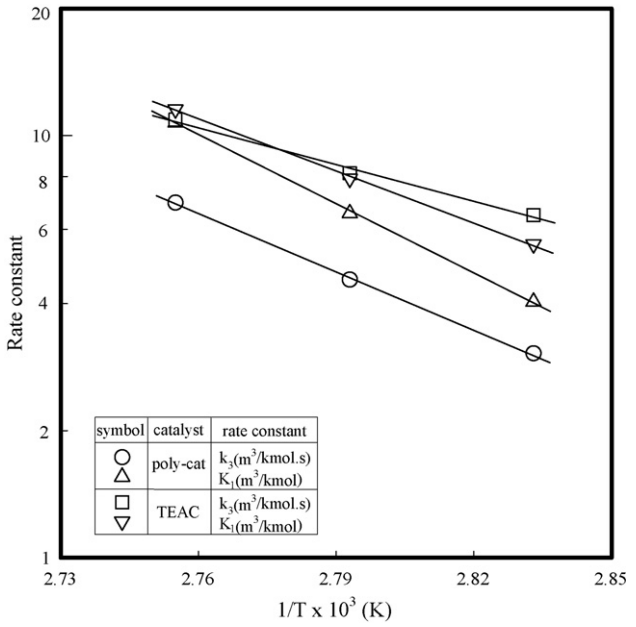

Fig. 8. Dependence of reaction temperature on reaction rate constant in DMSO solution.

are smaller than those for TEAC. The activation energy of reaction (3) for TEAC and the heat of reaction (2) are 13.2 and 18.59 kcal/mol, respectively. It is generally known that immobilized quaternary salt catalysts have lower catalytic activity than homogeneous ones [9] as shown in this study. However, the distinct comparison of the reactivity of homogeneous and immobilized quaternary salt catalysts is not easy since the structure of cation and counter anion of the catalyst greatly affects the catalytic performance.

As mentioned above, this work was done to suggest the application of the mass transfer phenomenon to the reaction kinetics in the heterogeneous systems such as CO_2/GMA.

5. Conclusions

The overall reaction between CO_2 and GMA using immobilized TEAC as a catalyst was assumed to consists of two elementary reactions: the reversible reaction of GMA and the catalyst to form an intermediate, and an irreversible reaction of this intermediate with carbon dioxide to form five-membered cyclic carbonate. Initial absorption rate of CO_2 was used to obtain the reaction rate constant of the elementary reaction and the concentration profile of each component in the liquid film from the numerical solution of the diffusion equations accompanied by the elementary reactions. Solubility parameter of solvent influenced on the reaction rate constants.

Acknowledgment

This work was supported from the Basic Research Program of the Korea Science and Engineering Foundation (KOSEF) through the Applied Rheology Center (ARC) and the Brain Korea 21 Project.

References

[1] M. Aresta, Carbon Dioxide Recovery and Utilization, Kluwer Academic Publishers, London, 2003.
[2] K. Weissermel, H. Arpe, Industrial Organic Chemistry, Wiley–VCH, Weinheim, 1997.
[3] W.J. Peppel, Ind. Eng. Chem. 50 (1950) 767.
[4] G. Rokicki, Makromol. Chem. 186 (1985) 331.
[5] T. Aida, S. Inoue, J. Am. Chem. Soc. 105 (1983) 1304.
[6] Y. Nishikubo, T. Kato, S. Sugimoto, M. Tomoi, S. Ishigaki, Macromolecules 23 (1990) 3406.
[7] N. Kihara, T. Endo, Macromolecules 25 (1992) 4824.
[8] T. Nishikubo, A. Kameyama, J. Yamashida, M. Tomoi, W. Fukuda, J. Polym. Sci. Part A: Polym. Chem. 31 (1993) 939.
[9] T. Nishikubo, A. Kameyama, J. Yamashida, T. Hukumitsu, C. Maejima, M. Tomoi, J. Polym. Sci. Part A: Polym. Chem. 33 (1995) 1011.
[10] C.M. Starks, C.L. Liotta, M. Halpern, Phase Transfer Catalysis, Chapmann & Hall, New York, 1994.
[11] L.K. Daraiswany, M.M. Sharma, Heterogeneous Reaction: Analysis, Example and Reactor Design, John Wiley & Sons, New York, 1980.
[12] S.W. Park, D.W. Park, T.Y. Kim, M.Y. Park, K.J. Oh, Catal. Today 98 (2004) 493.
[13] S.W. Park, B.S. Choi, D.W. Park, J.W. Lee, J. Ind. Eng. Chem. 11 (2005) 527.
[14] S.W. Park, J.W. Lee, Stud. Surf. Sci. Catal. 159 (2006) 345.
[15] S.W. Park, B.S. Choi, B.D. Lee, D.W. Park, S.S. Kim, Sep. Sci. Technol. 41 (2006) 829.
[16] D. Gomez-Diaz, J.C. Mejuto, J.M. Navaza, Chem. Eng. Sci. 61 (2006) 2330.
[17] B. Yu, E.S. Jeong, K.H. Kim, D.W. Park, S.W. Park, J.W. Lee, React. Kinet. Catal. Lett. 84 (2005) 175.
[18] M.L. Kennard, A. Meisen, J. Chem. Eng. Data 29 (1984) 309.
[19] P.V. Danckwerts, Gas–Liquid Reaction, McGraw-Hill Book Company, New York, 1970.
[20] S.W. Park, K.W. Kim, I.J. Sohn, Sep. Purif. Technol. 19 (2000) 43.
[21] H.F. Herbrandson, F.B. Neufeld, J. Org. Chem. 31 (1966) 1140.
[22] J. Brandrup, E.H. Immergut, Polymer Handbook, second ed., John Wiley & Sons, New York, 1975.
[23] R.T. Morrison, R.N. Boyd, Organic Chemistry, fourth ed., Allyn and Bacon, Inc., Toronto, 1983.